JOC Article

Natural Products, Stylissadines A and B, Specific Antagonists of the $P2X_7$ Receptor, an Important Inflammatory Target[1]

Malcolm S. Buchanan,[†] Anthony R. Carroll,[†] Rama Addepalli,[†] Vicky M. Avery,[†] John N. A. Hooper,[‡] and Ronald J. Quinn*,[†]

Natural Product Discovery, Eskitis Institute for Cell and Molecular Therapies, Griffith University, Nathan, Queensland 4111, Australia, and Queensland Centre for Biodiversity, Queensland Museum, South Brisbane, Queensland 4101, Australia

r.quinn@griffith.edu.au

Received September 28, 2006

Stylissa flabellata

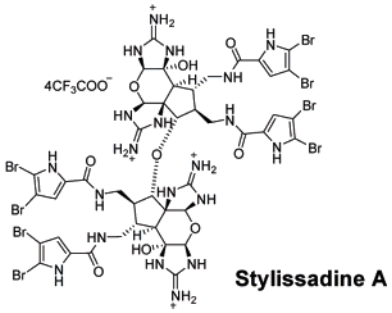

The distribution of the $P2X_7$ receptor in inflammatory cells suggests that $P2X_7$ antagonists have a significant role to play in the treatment of inflammatory disease. We conducted a natural product high-throughput screening campaign to discover $P2X_7$ receptor antagonists. The Australian marine sponge *Stylissa flabellata* yielded two new bisimidazo-pyrano-imidazole bromopyrrole ether alkaloids, stylissadines A (IC_{50} 0.7 μM) and B (IC_{50} 1.8 μM), as the specific bioactive constituents. The compounds inhibit BzATP-mediated pore formation in THP-1 cells. Also present in this extract was considerable nonspecific bioactivity in the hemeolysin specificity assay. A new pyrrole-imidazole alkaloid, konbu'acidin B, and the known pyrrole-imidazole alkaloids 4,5-dibromopalau'amine and massadine were also isolated and had nonspecific activity. ROESY and proton coupling constant data indicated that the stereochemistry at C12, C17, and C20 in 4,5-dibromopalau'amine should be revised to 12*R*, 17*S*, 20*S*. By analogy, the relative stereochemistry of palau'amine, 4-bromopalau'amine, styloguanidine, 3-bromostyloguanidine, and 2,3-dibromostyloguanidine should also be revised to 12*R*, 17*S*, 20*S*. Stylissadines A and B are the most potent natural product $P2X_7$ antagonists to be isolated to date and provide a novel class of $P2X_7$ receptor inhibitors. They are also the first examples of tetrameric pyrrole-imidazole alkaloids.

Introduction

This paper reports on the results of a natural product high-throughput screening (HTS) campaign to discover selective $P2X_7$ receptor (ligand gated cation channel) antagonists for the treatment of the inflammatory diseases, osteoarthritis, rheumatoid arthritis, or COPD. The $P2X_7$ receptor is activated by ATP, and with prolonged exposure to ATP, the opening of large plasma membrane pores occurs.[2,3] This leads to a rapid nonselective influx of cations as well as hydrophilic molecules with a molecular mass up to 900 Da. The physiological function

* To whom correspondence should be addressed. Phone: +61 7 3735 6006. Fax: +61 7 3735 6001.
[†] Griffith University.
[‡] Queensland Museum.

(1) After submission of this manuscript and presentation in part at the International Conference on Biodiversity and Natural Products, ICOB-5 & ISCNP-25 IUPAC, Kyoto, Japan, July 23−28, 2006, we learned of the publication by Grube and Köck published on the web September 23, 2006 (Grube, A.; Köck, M. *Org. Lett.* **2006**, *8*, 4675−4678). Our flabellazoles A and B were identical to stylissadines B and A, respectively. We acknowledge the precedence of stylissadines A and B.

(2) Baraldi, P. G.; De Carmen Nuñez, M.; Morelli, A.; Falzoni, S.; Di Virgilio, F.; Romagnoli, R. *J. Med. Chem.* **2003**, *46*, 1318−1329.
(3) Alcaraz, L.; Baxter, A.; Bent, J.; Bowers, K.; Braddock, M.; Cladingboel, D.; Donald, D.; Fagura, M.; Furber, M.; Laurent, C.; Lawson, M.; Mortimore, M.; McCormick, M.; Roberts, N.; Robertson, M. *Bioorg. Med. Chem. Lett.* **2003**, *13*, 4043−4046.

10.1021/jo062007q CCC: $37.00
Published on Web 02/22/2007

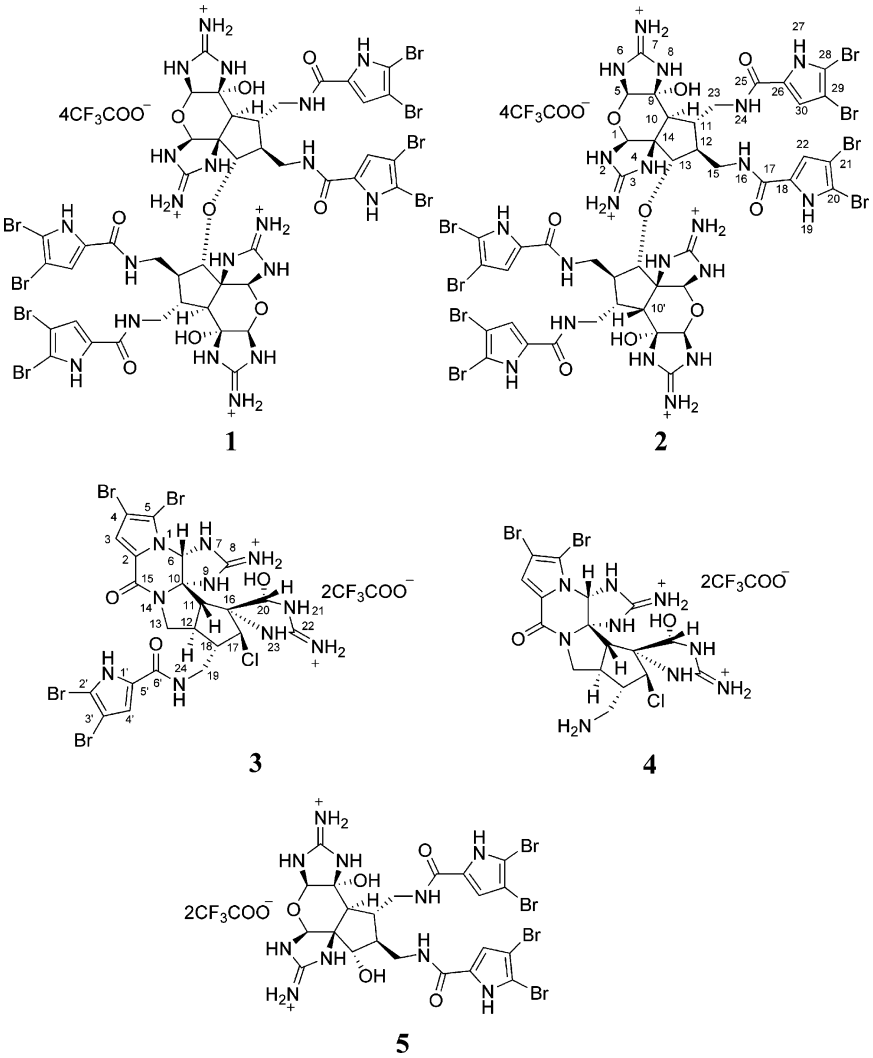

of $P2X_7$ is as yet unknown; however, its high expression in inflammatory and immunomodulatory cells, including microglia, macrophages, lymphocytes, and dendritic cells, where it mediates several relevant processes (cytokine release, NO generation, killing of intracellular pathogens, cytotoxicity), suggests that it may have an important role in inflammation and immunomodulation. Its most notable biological function is the processing and release of the proinflammatory cytokine interleukin-1β (IL-1β) from monocytes, macrophages, and microglial cells. IL-1β is an important inducer of immune and inflammatory responses. Mice genetically modified to have the $P2X_7$ receptor "knocked out" have been reported to show a reduced severity of arthritis.[4] Therefore, the objective of this HTS campaign was to identify antagonists of the $P2X_7$ receptor, which could be used as lead compounds for the development of antiinflammatory drugs. There have been several studies, which have reported the synthesis[2,3,5−9] of $P2X_7$ antagonists; however, thus far, the only reported natural product inhibitors are the benzophenanthridine alkaloids chelerythrine, sanguinarine, and berberine.[10]

The Australian marine sponge *Stylissa flabellata* Ridley & Dendy 1886 (Dictyonellidae) yielded two bisimidazo-pyrano-imidazole bromopyrrole ether alkaloids, stylissadines A (**1**) and B (**2**),[1] as the specific bioactive constituents. Also present in this extract was considerable nonspecific bioactivity, which was measured using a counter assay in which hemeolysin,[11] a nonspecific pore former, was used. The new pyrrole-imidazole konbu'acidin B (**3**) and the known pyrrole-imidazole alkaloids 4,5-dibromopalau'amine (**4**)[12] and massadine (stylissadine) (**5**)[13,14] were also isolated and had nonspecific activity. It has

(4) Labasi, J. M.; Petrushova, N.; Donovan, C.; McCurdy, S.; Lira, P.; Payette, M. M.; Brissette, W.; Wicks, J. R.; Audoly, L.; Gabel, C. A. *J. Immunol.* **2002**, *168*, 6436−6444.

(5) Duplantier, A. J.; Subramanyam, C.; Dombroski, M. A. PCT Int. Appl., 2004; Vol. WO 2004058731, CAN 141:123633.

(6) Jacobson, K. A. PCT Int. Appl., 2003; Vol. WO 2003047515, CAN 139:53304.

(7) Ravi, R. G.; Kertesy, S. B.; Dubyak, G. R.; Jacobson, K. A. *Drug Dev. Res.* **2001**, *54*, 75−87.

(8) Merriman, G. H.; Ma, L.; Shum, P.; McGarry, D.; Volz, F.; Sabol, J. S.; Gross, A.; Zhao, Z.; Rampe, D.; Wang, L.; Wirtz-Brugger, F.; Harris, B. A.; Macdonald, D. *Bioorg. Med. Chem. Lett.* **2005**, *15*, 435−438.

(9) Romagnoli, R; Baraldi, P. G.; Di Virgilio, F. *Expert Opin. Ther. Pat.* **2005**, *15*, 271−287.

(10) Shemon, A. N.; Sluyter, R.; Conigrave, A. D.; Wiley, J. S. *Br. J. Pharmacol.* **2004**, *142*, 1015−1019.

(11) Menestrina, G.; Dalla Serra, M.; Comai, M.; Coraiola, M.; Viero, G.; Werner, S.; Colin, D. A.; Monteil, H.; Prévost, G. *FEBS Lett.* **2003**, *552*, 54−60.

(12) Kinnel, R. B.; Gehrken, H.-P.; Swali, R.; Skoropowski, G.; Scheuer, P. J. *J. Org. Chem.* **1998**, *63*, 3281−3286.

(13) Nishimura, S.; Matsunaga, S.; Shibazaki, M.; Suzuki, K.; Furihata, K.; van Soest, R. W. M.; Fusetani, N. *Org. Lett.* **2003**, *5*, 2255−2257.

(14) Watanabe, M.; Fusetani, N.; Matsunaga, S.; Hishimura, S. Jpn. Kokai Tokkyo Koho, 2004; Vol. JP 2004059542, CAN 140:193034.

TABLE 1. ^{1}H (600 MHz) and ^{13}C (125 MHz) NMR Data for Stylissadine B (2) in DMSO-d_6

position	δ_C	δ_H (mult, *J* in Hz)	position	δ_C	δ_H (mult, *J* in Hz)
1	82.4 d	5.98 (s)	1′	79.3 d	5.61 (s)
2 (N)		9.27 (brs)	2′ (N)		9.21 (m)[h]
3	157.35 s[a]		3′	156.7 s	
4 (N)		9.21 (m)[h]	4′ (N)		9.25 (m)[i]
5	90.0 d	5.41 (d, 1.2)	5′	86.5 d	5.24 (s)
6 (N)		9.40 (brs)	6′ (N)		9.34 (brs)
7	157.38 s[a]		7′	156.9 s	
8 (N)		9.25 (m)[i]	8′ (N)		9.25 (m)[i]
9	87.0 s		9′	84.9 s	
10	45.7 d[b]	2.16 (d, 12.0)	10′	42.3 d	2.88 (brd, 9.0)
11	40.9 d	2.09 (brdq, 12.0, 7.0)	11′	38.8 d	2.21 (m)
12	50.1 d	1.87 (m)	12′	45.7 d[b]	1.94 (m)
13	83.7 d	3.79 (s)	13′	84.7 d	3.72 (m)
14	69.8 s		14′	68.3 s	
15	41.5 t	3.57 (m)a	15′	40.4 t	3.18 (m)a
		3.26 (m)b			3.07 (m)b
16 (N)		8.25 (brs)	16′ (N)		8.11 (brs)
17	159.8 s		17′	159.5 s	
18	127.66 s[c]		18′	127.63 s[c]	
19 (N)		12.52 (brs)	19′ (N)		12.50 (brd, 2.0)
20	105.1 s		20′	104.6 s[g]	
21	98.0 s[d]		21′	98.07 s[d]	
22	113.0 d	6.92 (d, 2.0)	22′	113.1 d	6.81 (s)[j]
23	43.5 t	3.62 (m)a	23′	40.1 t	3.50 (m)a
		3.16 (m)b			3.35 (m)b[k]
24 (N)		8.05 (m)	24′ (N)		8.04 (m)
25	158.9 s[e]		25′	158.6 s[e]	
26	128.0 s[f]		26′	128.0 s[f]	
27 (N)		12.68 (brs)	27′ (N)		12.36 (brs)
28	104.8 s		28′	104.3 s[g]	
29	98.1 s[d]		29′	98.11 s[d]	
30	112.2 d	6.77 (d, 2.0)	30′	112.5 d	6.81 (s)[j]
9-OH		7.90 (s)	9-OH′		7.43 (s)

[a−g] Interchangeable ^{13}C signals. [h−j] Overlapping ^{1}H signals. [k] Chemical shift determined from 2D experiments as ^{1}H signal obscured by H_2O.

been well documented that the biogenetic building block for the pyrrole-imidazole alkaloids is oroidin.[15] Massadine (**5**), originally known as stylissadine, was previously isolated from the marine sponge *Stylissa* aff. *massa* and is a pyrrole-imidazole dimer consisting of two oroidin skeletons sharing a hexasubstituted cyclopentane ring. Stylissadine A (**1**) was the ether-linked dimer of **5**. Further pyrrole-imidazole alkaloids previously isolated from *Stylissa* sp. were hymenin from *Stylissa massa*;[16] ageliferin, dibromoisophakellin, and *N*-methyldibromoisophakellin from *Stylissa caribica*;[17] and debromostevensine and debromohymenin from *Stylissa carteri*.[18] The *Stylissa* metabolites, latonduines A and B, the pyrrole-pyrimidine alkaloids from *Stylissa carteri*,[19] and the aldisine pyrrole-imidazolone alkaloids from *Stylissa massa*[16] appear to be related to the oroidin alkaloids, but alternative biogenetic pathways have been proposed.[19] Compound **4** is the dibromo analogue of palau'amine. Palau'amine and its related metabolites continue to be a synthetic challenge to several research groups, with over 30 papers published relating to this work.[15] It is their demanding structural complexity and interesting biological activity which have attracted considerable attention among the synthetic community. In this paper, we also report the structural revision of palau'amine.

Results and Discussion

Compounds **1**−**5** were discovered through HTS of a natural product extract library (62 749 extracts) against a functional readout of the P2X$_7$ receptor expressed endogenously on the human premonocytic cell line, THP-1. The biological screen for the determination of P2X$_7$ receptor inhibition was the reduction of plasma membrane pore formation stimulated by the synthetic ATP analogue, benzoylbenzoyl adenosine triphosphate (BzATP). Upon pore formation by BzATP, the membrane-impermeable nucleic acid stain Sytox Orange enters the cell through the pores and binds to nucleic acids resulting in an increase in fluorescence. Compounds disrupting pore formation inhibit cellular uptake of the dye giving decreased fluorescence. To determine nonspecific compound inhibition, a similar assay was used where BzATP was replaced with the nonspecific pore-forming compound hemeolysin. A dichloromethane/methanol (4:1) extract of the marine sponge *Stylissa flabellata* was shown to inhibit P2X$_7$ at a concentration equivalent of 0.17 μg/μL. Bioassay guided purification of this extract was achieved with several C_{18} HPLC purification steps using 1% TFA/H_2O/methanol. Extensive chromatography was required to separate the P2X$_7$-specific compounds from the extract, which contained many nonspecific constituents. This resulted in the isolation of the P2X$_7$-specific components, stylissadines A (**1**) and B (**2**), separated from nonspecific constituents, which included konbu'acidin B (**3**), 4,5-dibromopalau'amine (**4**), and massadine (**5**).

(15) Jacquot, D. E. N.; Lindel, T. *Curr. Org. Chem.* **2005**, *9*, 1551−1565.
(16) Tasdemir, D.; Mallon, R.; Greenstein, M.; Feldberg, L. R.; Kim, S. C.; Collins, K.; Wojciechowicz, D.; Mangalindan, G. C.; Concepcion, G. P.; Harper, M. K.; Ireland, C. M. *J. Med. Chem.* **2002**, *45*, 529−532.
(17) Assmann, M.; van Soest, R. W. M.; Koeck, M. *J. Nat. Prod.* **2001**, *64*, 1345−1347.
(18) Eder, C.; Proksch, P.; Wray, V.; Steube, K.; Bringmann, G.; van Soest, R. W. M.; Sudarsono; Ferdinandus, E.; Pattisina, L. A.; Wiryowidagdo, S.; Moka, W. *J. Nat. Prod.* **1999**, *62*, 184−187.
(19) Linington, R. G.; Williams, D. E.; Tahir, A.; van Soest, R.; Andersen, R. J. *Org. Lett.* **2003**, *5*, 2735−2738.

TABLE 2. gCOSY and gHMBC Data for Stylissadine B (2)

H	COSY (H no.)	$^{2,3}J_{CH}$ HMBC (C no.)	H	COSY (H no.)	$^{2,3}J_{CH}$ HMBC (C no.)
1	2	5, 13	1′		3′, 5′, 13′
2 (N)	1		2′ (N)		
3			3′		
4 (N)			4′ (N)		
5	6	1, 9	5′	6'	1', 7'
6 (N)	5	9	6′ (N)	5'	
7			7′		
8 (N)			8′ (N)		
9			9′		
10	11	9, 11, 14, 23	10′	11′	14′
11	10, 12, 23a, 23b	12, 15, 23	11′	10′, 12′, 23a′	
12	11, 15a, 15b		12′	11′, 13′, 15a′	
13		13′, 11, 14, 15	13′	12′	13, 1′, 14′
14			14′		
15a	12, 15b, 16		15a′	12′, 15b′, 16′	11′, 17′
15b	12, 15a, 16	13, 17	15b′	15a′, 16′	
16 (N)	15a, 15b		16′ (N)	15a′, 15b′	
17			17′		
18			18′		
19 (N)	22		19′ (N)		
20			20′		
21			21′		
22	19	20	22′		
23a	11, 23b, 24		23a′	11′, 24′	
23b	11, 23a, 24		23b′	24′	
24 (N)	23a, 23b		24′ (N)	23a′, 23b′	
25			25′		
26			26′		
27 (N)	30	30	27′ (N)		
28			28′		
29			29′		
30	27	28	30′		
9-OH		9	9-OH′		5′, 9′, 10′

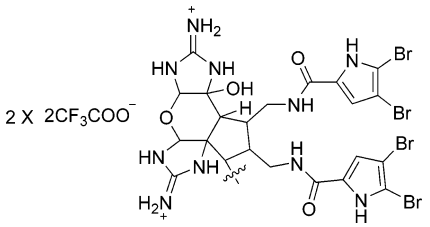

FIGURE 1. Partial structures for stylissadine B (**2**) (two massadine units).

The structure of stylissadine B (**2**) was determined from 1D and 2D NMR data (Table 1) and MS analysis. Compound **2** had a molecular formula determined to be $C_{44}H_{46}Br_8N_{20}O_9 \cdot 4CF_3COOH$ from HRESIMS. The positive electrospray mass spectrum of **2** displayed a cluster of ion peaks $[(M + 2H) - 4CF_3COOH]^{2+}$ at *m*/*z* 817/818/819/820/821/822/823. The intensities of the outer ions, *m*/*z* 816 and 824, in the Br_8 isotope pattern were too weak to be observed.

Examination of the ^1H and ^{13}C NMR data (Table 1) revealed that **2** had a doubling of resonances which were very similar to the known compound, massadine (**5**),[13,14] which was also present in this extract. Analysis of the 2D NMR data (Table 2) confirmed that **2** possessed two partial structures, which had identical planar structures, and these were almost identical to massadine (**5**) (Figure 1). Stereochemical differences in these partial structures may have accounted for their nonequivalence. Thus, the following moieties were identified: four 2-iminoimidazole units {δ_C 157.35, 157.38, 156.7, and 156.9; δ_H 9.21 (2H), 9.25 (3H), 9.27, 9.34, 9.40}, six tetrahydropyran methines (δ 42.3/2.88, 45.7/2.16, 79.3/5.61, 82.4/5.98, 86.5/5.24, 90.0/5.41) and four tetrahydropyran quaternary carbons {δ_C 68.3, 69.8, 84.9, 87.0), two hydroxyl protons (δ_H 7.90, 7.43), and four 4,5-dibromo-1*H*-pyrrole-2-carboxamide-*N*-CH_2- groups {carbonyls, δ_C 158.6, 158.9, 159.5, 159.8; pyrrole methines, δ_H 6.77, 6.81 (2H), 6.92; pyrrole NH's, δ_H 12.36, 12.50, 12.52, 12.68}. Furthermore, proton coupling constants and gCOSY correlations indicated that two partial structures of R−CH(O)−CH(CH_2-NH)−CH(CH_2NH)−CH−R were present. HMBC correlations allowed these moieties to be constructed into two massadine units (Figure 1). The MS data dictated that the molecule contained an oxygen atom linking the two massadine units together through an ether oxygen at C13 and C13′. This ether linkage was supported by gHMBC correlations observed between H13 (δ_H 3.79) and C13′ (δ_C 84.7) and between H13′ (δ_H 3.72) and C13 (δ_C 83.7). This completed the planar structure for compound **2**.

The relative stereochemistry was determined from proton coupling constants (Table 1) and correlations observed in a ROESY spectrum (Figure 2). Coupling constants of 12.0 Hz between H10 and H11, of 7.0 Hz between H11 and H12, and of 0 Hz between H12 and H13, supported by a ROESY correlation between H10 and H12, indicated that H10 and H12 were on the same face of the five-membered ring and that H11 and H13 were on the other face. Furthermore, there were no ROESY correlations between H1 and H5 and there was a correlation between H5 and 9-OH. From this, it was concluded that the C10−C14 ring junction was trans and that the tetrahydropyran ring was in a boat conformation, with the two iminoimidazo units running almost parallel (endo) to each other (Figure 2A). This stereochemistry and conformation was the same as that proposed for the same units in massadine (**5**).[13] Looking at the other half of the ether, the coupling constant of 9.0 Hz between H10′ and H11′, together with ROESY correla-

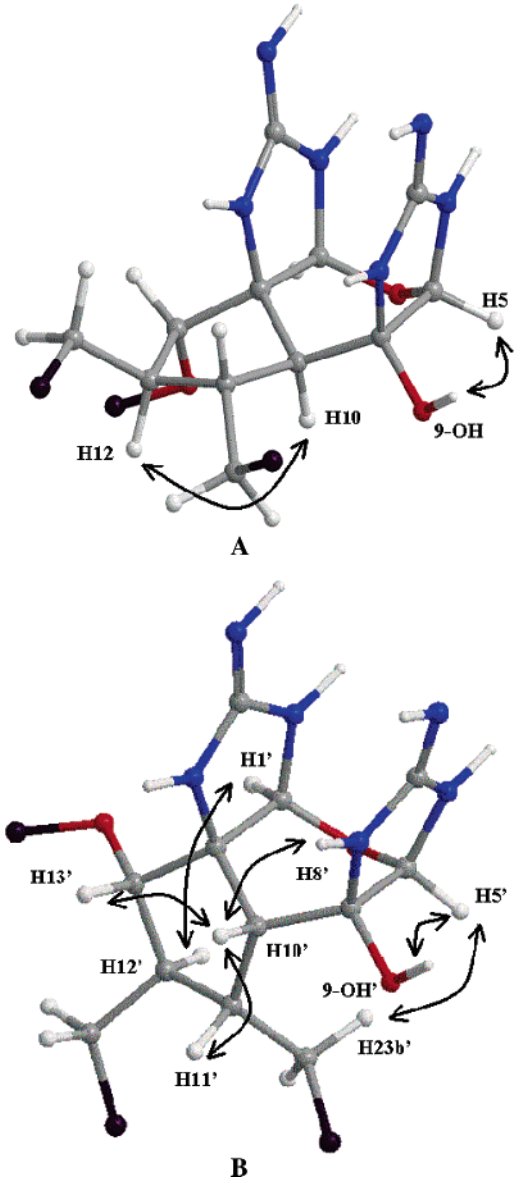

FIGURE 2. Proposed conformations of partial structures of stylissadine B (**2**) showing selected ROESY correlations.

tions from H10′ to H11′ and to H13′, indicated that H10′, H11′, and H13′ were on the same face of the five-membered ring and that H12′ was on the other face. Again, there were no ROESY correlations between H1′ and H5′ and there were correlations from H5′ to 9-OH′ and H23b′, from H10′ to H8′, and from H1′ to H12′. For this half of the molecule, it was concluded that the C10′−C14′ ring junction was cis and, as with the other half, that the tetrahydropyran ring was in a boat conformation, with the two iminoimidazo units running almost parallel to each other (Figure 2B). The only structural difference between both halves of the ether was the stereochemistries at C10 {δ_C 45.7; δ_H 2.16 (d, 12.0)} and C10′ {δ_C 42.3; δ_H 2.88 (brd, 9.0)} which were opposite. Hence, stylissadine B was the bisimidazo-pyrano-imidazole bromopyrrole ether alkaloid with structure **2**.

Stylissadine A (**1**) was isomeric with stylissadine B (**2**) and thus also had the molecular formula $C_{44}H_{46}Br_8N_{20}O_9$•$4CF_3$-COOH as determined from HRESIMS. The ^{1}H and ^{13}C NMR spectra of stylissadine A (**1**) (Table 3) contain half the number of signals compared to **2** indicating an axis of symmetry in the molecule. The spectra were also very similar to the spectra reported for massadine (**5**).[13,14] This suggested stylissadine A (**1**) differed from **2** only in the stereochemistry at C10′. Moreover, in **1**, the stereochemistry at C10 and C10′ was identical {δ_C 45.4; δ_H 2.21 (d, 12.0)}. Stylissadine A was also a bisimidazo-pyrano-imidazole bromopyrrole ether alkaloid and was assigned structure **1**, the ether-linked dimer of **5**.

The absolute stereochemistry of stylissadines A (**1**) and B (**2**) was assigned on the basis of the exciton chirality method in CD spectrometry.[20] This was also the method used for massadine (**5**).[13] The CD spectra of **1** {291 nm ($\Delta\epsilon$ +6.37) and 267 nm ($\Delta\epsilon$ −5.76)} and **2** {287 nm ($\Delta\epsilon$ +11.22) and 265 nm ($\Delta\epsilon$ −7.58)} both showed a positive exciton split due to the exciton coupling between the transition moments of the 4,5-dibromopyrrole-2-carboxyamide side chains. Thus, 11*R*, 12*R*, 11′*R*, 12′*R* stereochemistry was assigned and the absolute stereochemistry depicted for **1** and **2** was established.

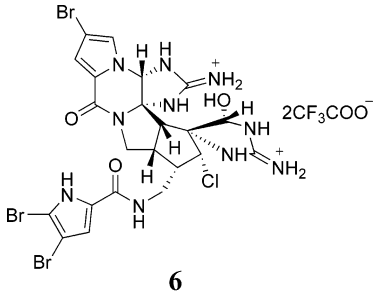

6

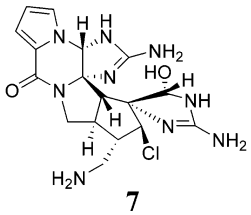

7

Konbu'acidin B (**3**) had the molecular formula $C_{22}H_{21}Br_4$-$ClN_{10}O_3$•$2CF_3COOH$ as analyzed by HRESIMS. The positive electrospray mass spectrum of **3** displayed a cluster of ion peaks $[(M + H) - 2CF_3COOH]^+$ at *m*/*z* 825/827/829/831/833/835 which was consistent with a $ClBr_4$ isotope pattern. Compound **3** was isolated in too small an amount (1.1 mg) for a 1D ^{13}C NMR spectrum to be obtained, thus ^{13}C chemical shifts were obtained from 2D NMR experiments. The ^{1}H and ^{13}C NMR spectral data (Table 4) for **3** indicated that it was closely related to konbu'acidin A (**6**).[21] Thus, there were resonances for two 2-iminoimadazole units {δ_C 156.8, 157.1; δ_H 7.91 (2H), 8.04 (2H), 8.68, 9.25, 9.65, 9.79}, a 4,5-dibromo-1*H*-pyrrole-2-carboxamide-*N*-CH_2− {δ_C 159.1 (C6′); δ_H 12.71 (H1′), 8.31 (H24), 6.95 (H4′)}, a chlorinated methine (δ_C 73.4; δ_H 4.33), a methine between two heteroatoms (δ_C 82.0; δ_H 5.69), and an α,*β*-unsaturated amide {δ_C 154.0 (C15)}. The fused pyrrole ring was 4,5-dibromo in **3** {δ_C 106.0 (C5)} compared with 4-monobromo in **6** {δ_C 123.8 (C5); δ_H 7.28 (H5)}. Furthermore, the stereochemistry at C12 and C17 in **3** was opposite to that in **6**. Thus, the octahydrocyclopenta[*c*]pyrrole ring system was trans fused in **3**. This was supported by the large coupling constant

(20) Nakanishi, K.; Berova, N.; Woody, R. W. *Circular Dichroism, Principles and Applications*; Wiley-VCH Publishers, Inc.: New York, 2000.
(21) Kobayashi, J.; Suzuki, M.; Tsuda, M. *Tetrahedron* **1997**, *53*, 15681−15684.

TABLE 3. ^{1}H (600 MHz), ^{13}C (125 MHz), gCOSY, and gHMBC NMR Data for Stylissadine A (1) in DMSO-d_6

position	δ_C	δ_H (mult, J Hz)	COSY (H no.)	$^{2,3}J_{CH}$ HMBC (C no.)
1/1′	82.1 d[a]	5.45 (s)		3, 5
2/2′ (N)		9.16 (brs)[d]		
3/3′	157.4 s			
4/4′ (N)		9.05 (brs)		14
5/5′	90.2 d	5.35 (d, 2.4)		7, 9
6/6′ (N)		9.16 (brs)[d]		
7/7′	157.2 s			
8/8′ (N)		9.37 (brs)		5, 7
9/9′	86.9 s			
10/10′	45.4 d	2.21 (d, 12.0)	11	9, 14, 23
11/11′	41.0 d	2.13 (brdq, 12.0, 7.0)	10, 12, 23b	10, 15
12/12′	48.2 d	2.03 (brq, 7.0)	11, 15	23
13/13′	82.1 d[a]	3.49 (s)		10, 14, 15
14/14′	69.4 s			
15/15′	41.7 t	3.30 (m, 2H)[e]	12, 16	
16/16′ (N)		8.37 (brs)	15	17
17/17′	159.4 s			
18/18′	127.5 s			
19/19′ (N)		12.42 (brs)	22	
20/20′	104.9 s[b]			
21/21′	98.1 s[c]			
22/22′	113.1 d	6.90 (d, 2.4)	19	18
23/23′	42.8 t	3.65 (dt, 12.6, 7.0)a	23b, 24	10
		3.41 (m)b[f]	11, 23a, 24	
24/24′ (N)		8.14 (brs)	23a, 23b	25
25/25′	159.0 s			
26/26′	127.8 s			
27/27′ (N)		12.65 (brs)	30	30
28/28′	104.9 s[b]			
29/29′	98.1 s[c]			
30/30′	112.6 d	6.84 (d, 2.4)	27	26
9/9′-OH		7.73 (s)		9, 10

[a–c] Interchangeable ^{13}C signals. [d] Overlapping ^{1}H signals. [e–f] Chemical shift determined from 2D experiments as ^{1}H signal obscured by H_2O.

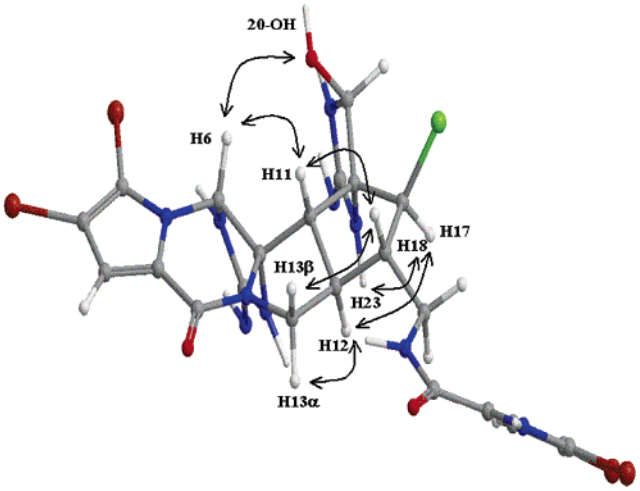

FIGURE 3. Selected ROESY correlations for konbu'acidin B (**3**).

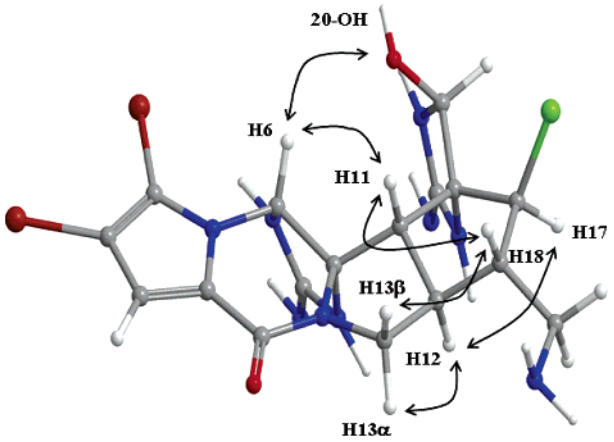

FIGURE 4. Selected ROESY correlations for compound **4**.

(13.8 Hz) between H11 and H12, together with information from a ROESY experiment (Figure 3). ROESY correlations from H18 to H11 and H13β placed them on the same face of the octahydrocyclopenta[*c*]pyrrole, and correlations from H12 to H17 and H13α placed them on the other face. Other significant ROESY correlations were from H6 to 20-OH and H11 and from H17 to H23. This placed H6 and H11 on the same face of the molecule and also established the stereochemistry at the spiro center (C16) and at C20. Therefore, konbu'acidin B was given structure **3**, with the absolute stereochemistry unassigned.

Compound **4** had ^{1}H and ^{13}C NMR data, together with an optical rotation {[α]$_D$ −110.7° (MeOH, *c* 0.11)}, which compared very well with those for the known compound 4,5-dibromopalau'amine[12] indicating that they were the same compound. However, the ROESY data for **4** (Figure 4) contradicted the relative stereochemistry published for 4,5-dibromopalau'amine. Compound **4** was an analogue of **3**. Whereas **3** had a 4,5-dibromo-1*H*-pyrrole-2-carboxamide moiety at N24, **4** had a primary amine. Similarly to **3**, ROESY correlations in **4** (DMSO-d_6) from H18 to H11 and H13β placed them on the same face of the octahydrocyclopenta[*c*]pyrrole, and correlations from H12 to H17 and H13α placed them on the other face. There were also ROESY correlations from H6 to 20-OH and H11. Therefore, in **4**, the octahydrocyclopenta[*c*]pyrrole ring system was trans fused (11*S*, 12*R*) with *S* stereochemistry at both C17 and C20, similar to **3**. However, the published structure

TABLE 4. ^{1}H (600 MHz), ^{13}C (125 MHz), gCOSY, and gHMBC NMR Data for Konbu'acidin B (3) in DMSO-d_6

position	δ_C[a]	δ_H (mult, *J* Hz)	COSY (H no.)	$^{2,3}J_{CH}$ HMBC (C no.)
2	124.8 s			
3	114.8 d	7.02 (s)		2, 5, 15
4	n.o.			
5	106.0 s			
6	67.9 d	6.41 (s)	7	8, 11
7 (N)		9.79 (s)	6	6, 8, 10
8	156.8 s			
8-NH_2		7.91 (brm, 2H)[b]		
9 (N)		9.65 (s)		6, 8
10	79.5 s			
11	55.1 d	3.03 (d, 13.8)	12	6, 10, 12, 16, 18, 20
12	40.0 d	2.48 (m)[c]	12, 13α	
13	44.7 t	3.85 (dd, 9.6, 7.2)α	12, 13*β*	11, 12
		3.02 (t, 9.6)*β*	12, 13α	
15	154.0 s			
16	70.4 s			
17	73.4 d	4.33 (d, 9.6)	18	16, 18, 19, 20
18	49.2 d	2.11 (m)	12, 17, 19a, 19b	
19	38.3 t	3.55 (dt, 14.4, 5.5)a	18, 19b, 24	6′, 12, 17
		3.40 (m)b[d]	18, 19a, 24	6′, 12, 17, 18
20	82.0 d	5.69 (brd, 4.8)	20-OH	17, 22
20-OH		7.67 (brd, 4.8)	20	16
21 (N)		9.25 (s)		16, 20, 22
22	157.1 s			
22-NH_2		8.04 (brm, 2H)[b]		
23 (N)		8.68 (s)		16, 20, 22
24 (N)		8.31 (t, 5.5)	19a, 19b	6′
1′		12.71 (brs)	4'	3′, 4′
2′	104.8 s			
3′	97.8 s			
4′	112.6 d	6.95 (d, 2.4)	1'	2′, 5′
5′	127.8 s			
6′	159.1 s			

[a] Chemical shifts determined from 2D NMR experiments. [b]Interchangeable ^{1}H signals. [c]Chemical shift determined from 2D NMR experiments as ^{1}H signal obscured by DMSO. [d]Chemical shift determined from 2D NMR experiments as ^{1}H signal obscured by H_2O. n.o. = not observed.

for 4,5-dibromopalau'amine depicted a cis-fused octahydrocyclopenta[*c*]pyrrole (11*S*, 12*S*) and *R* stereochemistry at both C17 and C20. The original paper[12] described the isolation and structure elucidation of palau'amine and deduced the structures of the 4-bromo and 4,5-dibromo analogues by comparison of spectral data. The stronger ROESY correlations published for palau'amine would also fit for **4**; however, most of the weak published correlations would not fit. The ROESY spectrum for palau'amine, included in the Supporting Information, suggested it may have been difficult to distinguish between noise and real correlations. Moreover, despite the dihedral angle between H11 and H12 being stated as 0.1° for palau'amine, there was no mention of a ROESY correlation between these two protons. Palau'amine, 4-bromopalau'amine, and 4,5-dibromopalau'amine all had the same relative stereochemistry, thus the above evidence suggests that the relative stereochemistry published for 4,5-dibromopalau'amine was incorrect and should be revised to that depicted in structure **4**. By analogy, the relative stereochemistry of palau'amine and 4-bromopalau'amine should also be corrected to 12*R*, 17*S*, 20*S*. Furthermore, in the same paper,[12] and also reported by Kato et al.,[22] the structures of regioisomers styloguanidine, 3-bromostyloguanidine, and 2,3-dibromostyloguanidine were described. They had NMR data nearly identical to those of palau'amine, 4-bromopalau'amine, and 4,5-dibromopalau'amine, respectively, except for the shifts of H6 and C6, which were shifted upfield by 0.7 and 10 ppm, respectively, and the pyrrole proton and carbon shifts differed to reflect the regioisomerism in ring A. Thus, although no NOE information was stated, it would be reasonable to also revise the relative stereochemistry of styloguanidine and its two bromo derivatives to 12*R*, 17*S*, 20*S*. The structural revision for palau'amine, represented in structure **7**, is especially significant considering its biological activities and its ongoing challenge to total synthesis.[15,23]

TABLE 5. Compounds 1−5 Inhibition of P2X$_7$ and Nonspecific Hemeolysin[a]

compound	P2X$_7$	hemeolysin[b]
stylissadine A (**1**)	0.7 μM	none
stylissadine B (**2**)	1.8 μM	none
konbu'acidin B (**3**)	3.0 μM	107% @ 100 μM
4,5-dibromopalau'amine (**4**)	40% @ 100 μM	−46% @ 100 μM
massadine (**5**)	64% @ 100 μM	66% @ 100 μM

[a] Assays performed in duplicate on three independent days. [b]Hemeolysin activity only given if >±30% at any concentration up to 100 μM.

Stylissadines A (**1**) and B (**2**) showed potent specific inhibition of P2X$_7$ at an IC$_{50}$ of 0.7 and 1.8 μM, respectively (Table 5). Konbu'acidin B (**3**), 4,5-dibromopalau'amine (**4**), and massadine (**5**) were nonspecific, showing bioactivity both against P2X$_7$ and in a hemeolysin specificity assay. It was interesting that **5** was a nonspecific antagonist of pore formation, whereas its ether-linked dimer, stylissadine A (**1**), was a specific antagonist for the P2X$_7$ receptor. Compounds **1**−**5** were not cytotoxic when screened in the Alamar Blue cytotoxicity assay for the incubation time of the P2X$_7$ assay. Current P2X$_7$

(22) Kato, T.; Shizuri, Y.; Izumida, H.; Yokoyama, A.; Endo, M. *Tetrahedron Lett.* **1995**, *36*, 2133−2136.

(23) Katz, J. D.; Overman, L. E. *Tetrahedron* **2004**, *60*, 9559−9568.

medicinal chemistry programs,[9] such as the optimization of KN-62, are obtaining analogues with low nanomolar IC_{50} values. Although stylissadines A (**1**) and B (**2**) are not as potent, they provide a novel class of $P2X_7$ antagonists available for optimization. Stylissadines A (**1**) and B (**2**) are interesting and useful tools to investigate the biology of $P2X_7$ antagonism, despite their large molecular weight and structural complexity which make them unattractive for further drug development. These two bisimidazo-pyrano-imidazole bromopyrrole ether alkaloids, stylissadines A (**1**) and B (**2**), are the most potent natural product $P2X_7$ antagonists isolated to date and are the first examples of tetrameric pyrrole-imidazole alkaloids.

Experimental Section

Animal Material. The sponge sample *Stylissa flabellata* (phylum Porifera, class Demospongiae, order Halichondrida, family Dictyonellidae) was collected by scuba diving at a depth of 15 m at Alcyonarian Point, Hook Island, Whitsundays, Queensland, Australia, in June 1999. A voucher sample, QMG314820, was lodged at the Queensland Museum, South Brisbane, Queensland, Australia.

Extraction and Isolation. The material was ground (75.6 g) and extracted sequentially with *n*-hexane, dichloromethane/MeOH (4:1), and finally MeOH. The dichloromethane/MeOH (4:1) extract (9.78 g) was further purified. A portion of the extract (1.11 g) was preabsorbed on C_{18} and loaded into two refillable preparative guard columns (30 mm × 10 mm i.d.), in line with a semipreparative C_{18} HPLC column. The following solvent conditions were used: H_2O/1% TFA to MeOH/1% TFA in 70 min, then isocratic for 50 min (flow rate of 5 mL/min); 60 fractions were collected. Fractions 21−34 were combined (468 mg) and purified further by C_{18} HPLC: H_2O/1% TFA to H_2O/1% TFA:MeOH/1% TFA (7:3) in 2 min, then to MeOH/1% TFA in 23 min, and finally isocratic for 5 min; 60 fractions were collected. Fractions 28 and 29 (93 mg) and fraction 41 (11.2 mg) were purified further by C_{18} HPLC. Fractions 28−29: H_2O/1% TFA to H_2O/1% TFA:MeOH/1% TFA (11:9) in 5 min, followed by isocratic for 15 min, then to MeOH/1% TFA in 5 min, and finally isocratic for 5 min; 60 fractions were collected. 4,5-Dibromopalau'amine (**4**) (8.8 mg, 0.2% dry wt) was eluted with a retention time of 16.4 min. Fraction 41: H_2O/1% TFA to H_2O/1% TFA:MeOH/1% TFA (7:13) in 5 min, followed by isocratic for 15 min, then to MeOH/1% TFA in 5 min, and finally isocratic for 5 min; 60 fractions were collected. Konbu'acidin B (**3**) (1.1 mg, 0.04% dry wt) was eluted with a retention time of 15.2 min. The remaining extract (8.67 g) was preabsorbed on C_{18} and loaded into a column (80 mm × 40 mm i.d.) in line with a preparative C_{18} HPLC column. The following solvent conditions were used: H_2O/1% TFA to MeOH/1% TFA in 50 min, then isocratic for 20 min (flow rate of 50 mL/min); 140 fractions were collected. Fractions 79−90 were combined (199 mg) and fractions 72−75 were combined (145 mg) and purified further by semipreparative C_{18} HPLC. Fractions 79−90 (199 mg): H_2O/1% TFA to H_2O/1% TFA:MeOH/1% TFA (3:7) in 5 min, then to MeOH/1% TFA in 18 min, and finally isocratic for 7 min; 60 fractions were collected. Fractions 27−39 were combined (83 mg) and purified further by C_{18} HPLC: H_2O/1% TFA:MeOH/1% TFA (1:1) to H_2O/1% TFA:MeOH/1% TFA (1:3) in 5 min, followed by isocratic for 15 min, and finally to MeOH/1% TFA in 10 min; 60 fractions were collected. Stylissadine B (**2**) (4.9 mg, 0.006% dry wt) was eluted with a retention time of 26.7 min, and stylissadine A (**1**) (2.6 mg, 0.003% dry wt) was eluted with a retention time of 24.8 min. Fractions 72−75 (145 mg): H_2O/1% TFA to H_2O/1% TFA:MeOH/1% TFA (7:13) in 5 min, followed by isocratic for 15 min, then to MeOH/1% TFA in 10 min; 60 fractions were collected. Fractions 43−45 were combined (9.5 mg) and purified further by C_{18} HPLC: H_2O/1% TFA:MeOH/1% TFA (2:3) isocratic for 40 min, then to MeOH/1% TFA in 10 min; 60 fractions were collected between 20 and 50 min. Massadine (**5**) (0.77 mg, 0.001% dry wt) was eluted with a retention time of 32.5 min. Compounds **1**−**5** were isolated as their trifluoroacetate salts.

Stylissadine A (1), *N*,*N*′,*N*″,*N*‴-(Oxybis{[(1*S*,2*R*,3*R*,3a*R*,6a*R*,-7a*S*,10a*S*,10b*R*)-10a-hydroxy-5,9-diiminodecahydro-1*H*-cyclopenta[3,4]imidazo[4′,5′:5,6]pyrano[2,3-*d*]imidazole-3,1,2-triyl]-bis(methylene)})tetrakis(4,5-dibromo-1*H*-pyrrole-2-carboxamide): isolated as an amorphous solid; $[\alpha]_D^{24}$ −22° (*c* 0.12, MeOH); UV (MeOH) λ_{max} (log ϵ) 277.5 (4.49) nm; CD (MeOH) λ_{ext} ($\Delta\epsilon$) 267 (−5.76), 278 (0.0), 291 (+6.37) nm; IR ν_{max} (film) 3167, 1675, 1632, 1567, 1528, 1203, 1139 cm^{-1}; ^1H and ^{13}C NMR, see Table 3; positive LRESIMS *m*/*z* 816.87 $[C_{44}H_{46}Br_7{}^{79}Br^{81}N_{20}O_9+2H]^{2+}$ (10), 817.86 $[C_{44}H_{46}Br_6{}^{79}Br_2{}^{81}N_{20}O_9+2H]^{2+}$ (35), 818.86 $[C_{44}H_{46}Br_5{}^{79}Br_3{}^{81}N_{20}O_9+2H]^{2+}$ (76), 819.86 $[C_{44}H_{46}Br_4{}^{79}Br_4{}^{81}N_{20}O_9+2H]^{2+}$ (100), 820.87 $[C_{44}H_{46}Br_3{}^{79}Br_5{}^{81}N_{20}O_9+2H]^{2+}$ (81), 821.87 $[C_{44}H_{46}Br_2{}^{79}Br_6{}^{81}N_{20}O_9+2H]^{2+}$ (41), 822.87 $[C_{44}H_{46}Br^{79}Br_7{}^{81}N_{20}O_9+2H]^{2+}$ (13); positive HRESIMS *m*/*z* 819.863046 $[C_{44}H_{46}Br_4{}^{79}Br_4{}^{81}N_{20}O_9+2H]^{2+}$ (calcd 819.864694, Δ −2.0 ppm).

Stylissadine B (2), *N*-{[(1*S*,2*R*,3*R*,3a*R*,6a*R*,7a*S*,10a*S*,10b*R*)-3{[(1*S*,2*R*,3*R*,3a*R*,6a*R*,7a*S*,10a*S*, 10b*S*)-1,2-Bis({[(4,5-dibromo-1*H*-pyrrol-2-yl)carbonyl]amino}methyl)-10a-hydroxy-5,9-diiminodo decahydro-1*H*-cyclopenta[3,4]imidazo[4′,5′:5,6]pyrano[2,3-*d*]imidazol-3-yl]oxy}-1-({[(4,5-dibromo-1*H*-pyrrol-2-yl)carbonyl]amino}methyl)-10a-hydroxy-5,9-diiminodecahydro-1*H*-cyclopenta[3,4]imidazo[4′,5′:5,6]pyrano[2,3-*d*]imidazol-2-yl]methyl}-4,5-dibromo-1*H*-pyrrole-2-carboxamide: isolated as an amorphous solid; $[\alpha]_D^{24}$ −20° (*c* 0.21, MeOH); UV (MeOH) λ_{max} (log ϵ) 277.5 (4.56) nm; CD (MeOH) λ_{ext} ($\Delta\epsilon$) 265 (−7.58), 277 (0.0), 287 (+11.22) nm; IR ν_{max} (film) 3192, 1679, 1632, 1530, 1325, 1205 cm^{-1}; ^1H and ^{13}C NMR, see Table 1; positive LRESIMS *m*/*z* 816.87 $[C_{44}H_{46}Br_7{}^{79}Br^{81}N_{20}O_9+2H]^{2+}$ (11), 817.87 $[C_{44}H_{46}Br_6{}^{79}Br_2{}^{81}N_{20}O_9+2H]^{2+}$ (36), 818.87 $[C_{44}H_{46}Br_5{}^{79}Br_3{}^{81}N_{20}O_9+2H]^{2+}$ (76), 819.86 $[C_{44}H_{46}Br_4{}^{79}Br_4{}^{81}N_{20}O_9+2H]^{2+}$ (100), 820.86 $[C_{44}H_{46}Br_3{}^{79}Br_5{}^{81}N_{20}O_9+2H]^{2+}$ (79), 821.86 $[C_{44}H_{46}Br_2{}^{79}Br_6{}^{81}N_{20}O_9+2H]^{2+}$ (40), 822.87 $[C_{44}H_{46}Br^{79}Br_7{}^{81}N_{20}O_9+2H]^{2+}$ (12); positive HRESIMS *m*/*z* 819.862438 $[C_{44}H_{46}Br_4{}^{79}Br_4{}^{81}N_{20}O_9+2H]^{2+}$ (calcd 819.864694, Δ −2.8 ppm).

Konbu'acidin B (3), 4,5-Dibromo-*N*-{[(3a*R*,10a*R*,11*R*,12*R*,-13*S*,13a*R*,13b*S*)-5,6-dibromo-12-chloro-5′-hydroxy-2,2′-diimino-8-oxo-1,2,3,3a,10a,11,12,13a-octahydro-8*H*,10*H*-spiro[cyclopenta-[3,4]pyrrolo[1,2-*a*]imidazo[4,5-*b*]pyrrolo[1,2-*d*]pyrazine-13,4′-imidazolidin]-11-yl]methyl}-1*H*-pyrrole-2-carboxamide: isolated as an amorphous solid; $[\alpha]_D^{24}$ −24° (*c* 0.04, MeOH); UV (MeOH) λ_{max} (log ϵ) 281.0 (3.91) nm; IR ν_{max} (film) 3170, 1678, 1642, 1531, 1277, 1205 cm^{-1}; ^1H and ^{13}C NMR, see Table 4; positive LRESIMS *m*/*z* 824.79 $[C_{22}H_{21}Br_4{}^{79}Cl^{35}N_{10}O_3+H]^+$ (15), 826.79 $[C_{22}H_{21}Br_3{}^{79}Br_1{}^{81}Cl^{35}N_{10}O_3+H]^+$ (62), 828.78 $[C_{22}H_{21}Br_2{}^{79}Br_2{}^{81}Cl^{35}N_{10}O_3+H]^+$ (100), 830.77 $[C_{22}H_{21}Br_2{}^{79}Br_2{}^{81}Cl^{37}N_{10}O_3+H]^+$ (77), 832.77 $[C_{22}H_{21}Br_1{}^{79}Br_3{}^{81}Cl^{37}N_{10}O_3+H]^+$ (29), 834.76 $[C_{22}H_{21}Br_4{}^{81}Cl^{37}N_{10}O_3+H]^+$ (4); positive HRESIMS *m*/*z* 832.823602 $[C_{22}H_{21}Br_1{}^{79}Br_3{}^{81}Cl^{37}N_{10}O_3+H]^+$ (calcd 832.821341, Δ +2.7 ppm), 830.827036 $[C_{22}H_{21}Br_2{}^{79}Br_2{}^{81}Cl^{37}N_{10}O_3+H]^+$ (calcd 830.823221, Δ +4.6 ppm).

General $P2X_7$ Assay Principle. THP-1 cells endogenously expressing the $P2X_7$ receptor were incubated with the potent $P2X_7$ receptor agonist 2′,3′-*O*-(4-benzoylbenzoyl) adenosine 5′-phosphate (BzATP) (selective for $P2X_7$) to produce pore formation and a cell membrane impermeable nucleic acid stain, Sytox Orange. Once the pore is open, Sytox Orange passes through the pore into the cell and binds nucleic acids which results in an increase in fluorescence.

General $P2X_7$ Assay Procedure. The test substances were added to microtiter plates. The three reagents, BzATP, THP-1 cells, and Sytox Orange, were dispensed consecutively into the 384 plate. The plate was incubated for 90 min at 37 °C and read on a fluorescence plate reader using 530 nm excitation and 620 nm emission wavelengths. The percentage inhibition was then calculated.

$P2X_7$ Assay Method. THP−1 cells were centrifuged twice (1570 rpm) and resuspended into high potassium solution (HKS) (consisting of 0.125 M KCl, 1 mM EDTA, 0.02 M HEPES free acid, 5

mM glucose made up to pH 7.4 with KOH) at a concentration of 5×10^5 cells/mL (15 000/well). Sytox Orange was added to the cell mix to give a 10 μM final solution (1:500 dilution) just before addition to the microtiter plate. BzATP in HKS was then added to each well to give a final concentration of 10 μM. The assay was performed in 384 microtiter plates and consisted of the following additions: 0.5 μL of compound (stock 10 mM in DMSO), 4.5 μL of water, 10 μL of BzATP, 30 μL of cells with Sytox Orange. In-plate controls consisted of 100% activity (0.5 μL of DMSO plus 10 μL of BzATP) and 0% activity (0.5 μL of DMSO plus 10 μL of HKS in place of BzATP). All plates were incubated at 37 °C for 90 min and read at 530 nm excitation and 620 nm emission on a fluorescence plate reader. Compound activity was expressed as percentage inhibition compared to the 100% activity control.

Acknowledgment. We thank AstraZeneca for financial support. We are indebted to Dr. Jennifer Mitchell, Griffith University, Brisbane, for HRESIMS analyses. We wish to thank Dr. Gregory Fechner for fruitful discussions pertaining to the biological assay. We also acknowledge Mr. Anthony Boyle for his small-scale chemistry work on extracts and Mr. David Pass for CD measurements.

Supporting Information Available: Experimental general procedures. Principle, procedure, and method for the hemeolysin and Alamar Blue cytotoxicity assays. ^{1}H, ^{13}C, gCOSY, and gHMBC NMR data in DMSO-d_6 and ^{1}H, ^{13}C, and gHMBC NMR data in D_2O for compound **4**. Figure giving ROESY spectrum of compound **4**. ^{1}H, ^{13}C, gCOSY, and gHMBC NMR data in DMSO-d_6 for compound **5**. Figures giving 1D and 2D NMR spectra for compounds **1**−**3**. This material is available free of charge via the Internet at http://pubs.acs.org.

JO062007Q